

## Electronic Structure of Co<sup>III</sup> Doped Bromo-Bridged Ni Complexes, [Ni<sub>1-x</sub>Co<sub>x</sub>(chxn)<sub>2</sub>Br]Br<sub>2</sub>

Jimin Xie,<sup>†</sup> Hashen Wu,<sup>†</sup> Daisuke Kawakami,<sup>†</sup> Hiroaki Iguchi,<sup>†</sup> Shinya Takaishi,<sup>†</sup> Masahiro Yamashita,<sup>\*,†</sup> Hiroyuki Matsuzaki,<sup>‡</sup> Hiroshi Okamoto,<sup>‡</sup> Hisaaki Tanaka,<sup>§</sup> and Shin-ichi Kuroda<sup>§</sup>

Department of Chemistry, Faculty of Science, Tohoku University & CREST(JST), Aramaki-Aza-Aoba, Aoba-ku, Sendai 980-8578, Japan, Department of Advanced Materials Science, Graduate School of Frontier Sciences, The University of Tokyo, Kashiwa 277-8561, Japan, and Department of Applied Physics, Graduate School of Engineering, Nagoya University, Nagoya 464-8603, Japan

Received June 22, 2007

This article describes the electronic structure of the Co<sup>III</sup> doped Br bridged Ni<sup>III</sup> complexes, [Ni<sub>1-x</sub>Co<sub>x</sub>(chxn)<sub>2</sub>Br]Br<sub>2</sub> ( $x = 0.01, 0.02, 0.05, \text{ and } 0.11$ ) by using a optical spectroscopy, scanning tunneling microscopy (STM), and electron spin resonance spectroscopy. In the optical reflectivity spectrum, the new band was formed at about 0.5 eV, which is reasonably recognized as the  $d_{z^2}$  band of doped Co<sup>III</sup> ions. In the STM images of [Ni<sub>1-x</sub>Co<sub>x</sub>(chxn)<sub>2</sub>Br]Br<sub>2</sub>, the bright spots attributable to the tunnel current from the Fermi level of the STM tip to the conduction band of the sample were observed. In addition, some brighter spots were also observed. Because the number of the brighter spots is in good agreement with that of doped Co species, the brighter spots can be assigned to doped Co<sup>III</sup> sites. These are reasonably explained by the tunnel current from the Fermi level of the tip to the  $d_{z^2}$  band of Co<sup>III</sup>. The Curie spin concentration was gradually increased with increasing Co<sup>III</sup> ions, which is explained by the scissions of the  $S = 1/2$  1D antiferromagnetic chains.

### Introduction

In recent years, quasi one-dimensional (1D) halogen-bridged mixed valence compounds (MX chains) have been attracting considerable attention because of their characteristic physical properties such as intense and dichroic inter-valence charge-transfer (CT) bands, overtone progressions of resonance Raman spectra, luminescence spectra with large

Stokes shifts, large third-order nonlinear optical properties, midgap absorptions attributable to solitons and polarons, and so forth, as well as providing the 1D model compounds of high  $T_c$  copper oxide superconductors.<sup>1</sup> Theoretically, these MX chains are considered as Peierls–Hubbard systems, where the electron–phonon interaction ( $S$ ), the electron transfer ( $T$ ), and the intra and intersite Coulomb repulsion energies ( $U$  and  $V$ , respectively) compete or cooperate with each other.<sup>2</sup> The halogen-bridged Pt and Pd compounds form charge-density wave (CDW) states or M<sup>II</sup>–M<sup>IV</sup> mixed-valence states because of the strong electron–phonon interaction ( $S$ ), where the bridging halogens are displaced from the midpoints between the neighboring two metal ions.<sup>3</sup> On the other hand, the halogen-bridged Ni compounds form the Ni<sup>III</sup>–Ni<sup>III</sup>Mott–Hubbard states because of the strong electron correlation ( $U$ ), where the bridging halogens are located at

\* To whom correspondence should be addressed. E-mail: yamasita@agnus.chem.tohoku.ac.jp.

<sup>†</sup> Tohoku University & CREST(JST).

<sup>‡</sup> The University of Tokyo.

<sup>§</sup> Nagoya University.

- (1) (a) Bishop, A. R.; Swanson, B. I. *Los Alamos Sci.* **1993**, *21*, 133–143. (b) Clark, R. J. H. *Adv. Infrared Raman Spectrosc.* **1983**, *11*, 95–132. (c) Clark, R. J. H.; Kurmoo, M.; Mountney, D. N.; Toftlund, H. *J. Chem. Soc., Dalton Trans.* **1982**, 1851–1860. (d) Okamoto, H.; Yamashita, M. *Bull. Chem. Soc. Jpn.* **1998**, *71*, 2023–2039. (e) Yamashita, M.; Manabe, T.; Kawashima, T.; Okamoto, H.; Kitagawa, H. *Coord. Chem. Rev.* **1999**, *190–192*, 309–330. (f) Iwasa, Y.; Funatsu, E.; Koda, T.; Yamashita, M. *Appl. Phys. Lett.* **1991**, *59*, 2219–2221. (g) Kuroda, N.; Sakai, M.; Nishina, Y.; Tanaka, M.; Kurita, S. *Phys. Rev. Lett.* **1987**, *58*, 2122–2125. (h) Okamoto, H.; Mitani, T.; Toriumi, K.; Yamashita, M. *Phys. Rev. Lett.* **1982**, *69*, 2248–2251. (i) *Extended Linear Chain Compounds*; Miller, J. S., Ed.; Plenum: New York, 1982; Vols. I–III.

- (2) (a) Nasu, K. *J. Phys. Soc. Jpn.* **1983**, *52*, 3865–3873. (b) Gammel, J. T.; Saxena, A.; Batstic, I.; Bishop, A. R.; Phillpot, S. R. *Phys. Rev. B.* **1992**, *45*, 6408–6434.

- (3) Hazell, A. *Acta Crystallogr., Sect. C* **1991**, *47*, 962–966.

the midpoints between the neighboring two Ni atoms.<sup>4</sup> Therefore, these compounds belong to the class III type of the Robin–Day classification for the mixed-valence complexes.<sup>5</sup> Quite strong antiferromagnetic interactions are acting among the spins located on the Ni<sup>III</sup>  $d_{z^2}$  orbital through the  $p_z$  orbital of the bridging halogen ions in these compounds.<sup>6</sup> Recently, a gigantic third-order nonlinear optical susceptibility ( $\chi^{(3)} \approx 10^{-4}$  esu) has been observed in  $[\text{Ni}(\text{chxn})_2\text{Br}]_2\text{Br}_2$  ( $\text{chxn} = 1R,2R$ -diaminocyclohexane).<sup>7</sup>

More recently, the local electronic structures, such as the Mott–Hubbard state, the CDW state, and the spin soliton of the mixed metal complexes  $[\text{Ni}_{1-x}\text{Pd}_x(\text{chxn})_2\text{Br}]_2\text{Br}_2$ , have been directly observed by using scanning tunneling microscopy (STM) for the first time.<sup>8</sup>

In the preceding paper, we have reported the incorporation of Co<sup>III</sup> ions into the Ni<sup>III</sup> complexes, that is,  $[\text{Ni}_{1-x}\text{Co}_x(\text{chxn})_2\text{Br}]_2\text{Br}_2$ .<sup>9</sup> The electron configuration of Co<sup>III</sup>( $d^6$ ) is different from that of Ni<sup>III</sup>( $d^7$ ). Therefore, the electronic states of Ni<sup>III</sup> mixed metal complexes doped by Co<sup>III</sup> ions are very interesting.

In this paper, we describe the electronic structures of these quasi 1D bromo-bridged Ni<sup>III</sup> mixed metal complexes measured by optical spectroscopy, electron spin resonance (ESR) spectroscopy, and STM.

## Experimental Section

We synthesized a series of single crystals of the complexes  $[\text{Ni}_{1-x}\text{Co}_x(\text{chxn})_2\text{Br}]_2\text{Br}_2$  by an electrolysis of a mixed solution of  $[\text{Ni}^{\text{III}}(\text{chxn})_2\text{Br}]_2\text{Br}_2$  (60 mM) and  $[\text{Co}^{\text{III}}(\text{chxn})_2\text{Br}]_2\text{Br}_2$  with tetra-*n*-butylammonium bromide (0.1 M). The elemental ratio of Ni and Co ions was determined with a Shimadzu ICPS-7510 ICP emission spectrometer. The polarized reflectivity spectrum was obtained by using a specially designed spectrometer equipped with a 25-cm grating monochromator, and an optical microscope. ESR spectra were measured by using a Bruker EMX spectrometer equipped with a gas-flow type cryostat Oxford ESR 900. STM measurements were performed at room temperature and ambient pressure with mechanically sharpened Pt/Ir tips. Single crystals of the present compounds were cleaved using a knife blade and mounted onto a sample stage with carbon pastes so as that the surface of  $bc$  plane can be observed. STM images were acquired with constant height mode using a JEOL JSPM-5200 microscope. A sample bias voltage ( $V_s$ ) was chosen to be +0.25 V.

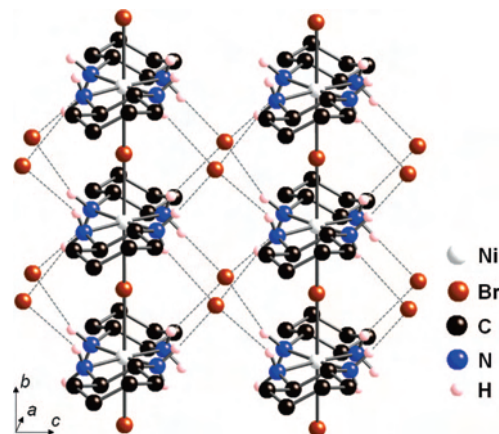


**Figure 1.** Crystal structure of  $[\text{Ni}(\text{chxn})_2\text{Br}]_2\text{Br}_2$ . Hydrogen atoms bonding to carbon atoms are omitted for clarity.

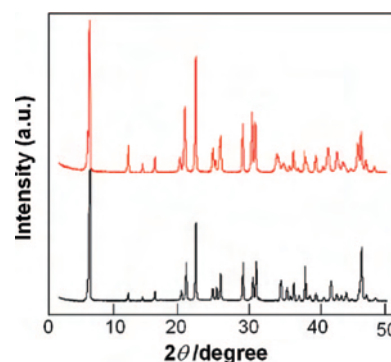


**Figure 2.** XRPD pattern of  $[\text{Ni}_{0.89}\text{Co}_{0.11}(\text{chxn})_2\text{Br}]_2\text{Br}_2$  (red line) together with that of  $[\text{Ni}(\text{chxn})_2\text{Br}]_2\text{Br}_2$  (black line).

## Results and Discussion

The crystal structure of  $[\text{Ni}(\text{chxn})_2\text{Br}]_2\text{Br}_2$  is shown in Figure 1.<sup>4</sup> In this structure, Ni<sup>III</sup> ions and bromide ions are arranged alternately along the  $b$  axis, forming the linear chain structures. Each Ni–Br–Ni chain is hydrogen-bonded between amino-hydrogen atoms of  $\text{chxn}$  and counter bromide ions along the chains, as well as over the chains, forming two-dimensional hydrogen-bond networks. However, the electronic structure of this compound is still 1D because the frontier orbitals are formed by the  $d_{z^2}$  orbital of Ni<sup>III</sup> ion and the  $p_z$  orbital of Br<sup>−</sup> ion. The Ni–Ni distances along the  $b$  (1D chain) and  $c$  axes are 5.16 Å and 7.12 Å, respectively. Figure 2 shows the X-ray powder diffraction (XRPD) pattern of  $[\text{Ni}_{1-x}\text{Co}_x(\text{chxn})_2\text{Br}]_2\text{Br}_2$  ( $x = 0.11$ ) together with that of  $[\text{Ni}(\text{chxn})_2\text{Br}]_2\text{Br}_2$ .  $[\text{Ni}_{1-x}\text{Co}_x(\text{chxn})_2\text{Br}]_2\text{Br}_2$  and  $[\text{Ni}(\text{chxn})_2\text{Br}]_2\text{Br}_2$  showed similar XRPD patterns to each other. Therefore, Co ions are successfully incorporated to  $[\text{Ni}(\text{chxn})_2\text{Br}]_2\text{Br}_2$ .

To clarify the electronic state of  $[\text{Ni}_{1-x}\text{Co}_x(\text{chxn})_2\text{Br}]_2\text{Br}_2$ , we measured single crystal polarized reflectivity spectrum of the crystal ( $x = 0.11$ ). The intensity of the peak at about 1.3 eV, which is attributable to the CT band from the bridging Br ions to the Ni ions, was drastically decreased, and a new band appeared at about 0.5 eV, as shown in Figure 3. This result suggests that some midgap state is formed by introducing Co ions.

Proposed schematic band structures of  $[\text{Ni}(\text{chxn})_2\text{Br}]_2\text{Br}_2$  and  $[\text{Ni}_{1-x}\text{Co}_x(\text{chxn})_2\text{Br}]_2\text{Br}_2$  are shown in Figure 4. Okamoto

- (4) Toriumi, K.; Wada, Y.; Mitani, T.; Bandow, S.; Yamashita, M.; Fujii, Y. *J. Am. Chem. Soc.* **1989**, *111*, 2341–2342.
- (5) Robin, M. B.; Day, P. *Adv. Inorg. Chem. Radiochem.* **1967**, *9*, 247–422.
- (6) Okamoto, H.; Toriumi, K.; Mitani, T.; Yamashita, M. *Phys. Rev. B* **1990**, *42*, 10381–10387.
- (7) Kishida, H.; Matsuzaki, H.; Okamoto, H.; Manabe, T.; Yamashita, M.; Taguchi, Y.; Yokoyama, K. *Nature* **2000**, *405*, 929–932.
- (8) Takaishi, S.; Miyasaka, H.; Sugiura, K.-i.; Yamashita, M.; Matsuzaki, H.; Kishida, H.; Okamoto, H.; Tanaka, H.; Marumoto, K.; Ito, H.; Kuroda, S.; Takami, T. *Angew. Chem., Int. Ed.* **2004**, *43*, 3171–3175.
- (9) Yamashita, M.; Yokoyama, K.; Furukawa, S.; Manabe, T.; Ono, T.; Nakata, K.; Kachi-Terajima, C.; Iwahori, F.; Ishii, T.; Miyasaka, H.; Sugiura, K.; Matsuzaki, H.; Kishida, H.; Okamoto, H.; Tanaka, H.; Hasegawa, Y.; Marumoto, K.; Ito, H.; Kuroda, S. *Inorg. Chem.* **2002**, *41*, 1998–2000.
- (10) Okamoto, H.; Shimada, Y.; Oka, Y.; Chainani, A.; Takahashi, T.; Kitagawa, H.; Mitani, T.; Toriumi, K.; Inoue, K.; Manabe, T.; Yamashita, M. *Phys. Rev. B* **1996**, *54*, 8438–8445.

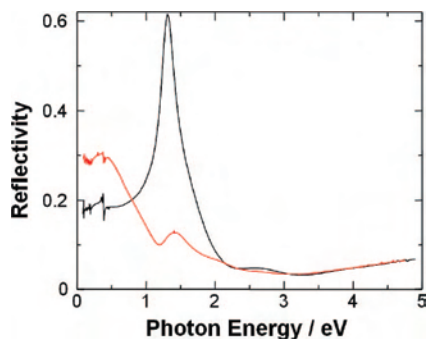


**Figure 3.** Optical reflectivity spectrum of  $[\text{Ni}_{0.89}\text{Co}_{0.11}(\text{chxn})_2\text{Br}]\text{Br}_2$  (red line) together with that of  $[\text{Ni}(\text{chxn})_2\text{Br}]\text{Br}_2$  (black line).

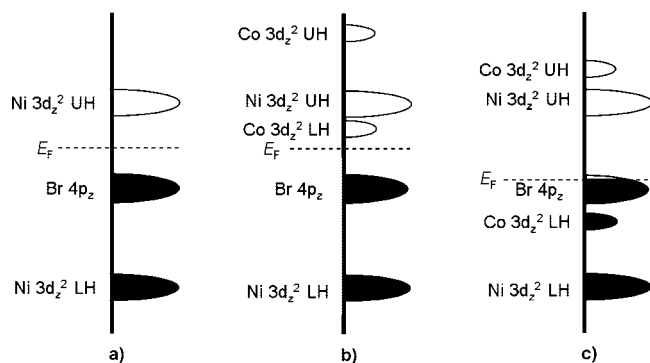


**Figure 4.** Schematic band structures of (a)  $[\text{Ni}^{\text{III}}(\text{chxn})_2\text{Br}]\text{Br}_2$ , (b)  $[\text{Ni}^{\text{III}}_{1-x}\text{Co}^{\text{III}}_x(\text{chxn})_2\text{Br}]\text{Br}_2$ , and (c)  $[\text{Ni}^{\text{III}}_{1-x}\text{Co}^{\text{II}}_x(\text{chxn})_2\text{Br}^{x-1}]\text{Br}_2$ .

et al. have revealed the band structure of  $[\text{Ni}(\text{chxn})_2\text{Br}]\text{Br}_2$  by using the X-ray photoelectron spectrum (XPS), Auger electron spectrum (AES), and optical conductivity spectrum.<sup>10</sup> From XPS and AES, the  $U$  value was estimated to be about 5.5 eV ( $U = E_{2p}(\text{XPS}) - 2E_{\text{valence}}(\text{XPS}) - E_{\text{K}}(\text{AES})$ ), which is much larger than that of the Pd ( $\sim 1.5$  eV)<sup>13</sup> or Pt ( $\sim 1.0$  eV)<sup>14</sup> systems. On the other hand, the optical conductivity spectra showed an intense CT band at 1.3 eV, which is attributable to CT from the bridging halide ions to the upper Hubbard band of Ni. Therefore, the band structure can be schematically illustrated as in Figure 4a. In  $[\text{Ni}_{1-x}\text{Co}_x(\text{chxn})_2\text{Br}]\text{Br}_2$ , on the other hand, the main peak at 1.3 eV was drastically decreased, and a new band appeared at about 0.5 eV by doping Co as shown in Figure 3. We can consider the two possible band structures as shown in Figure 4b,c. One possibility is that the energy level of the  $d_{z^2}$  LH band of Co is higher than that of the  $p_z$  band of the bridging Br (Figure 4b). In this case, Co ions are in the  $d^6$  (trivalent) state, and these compounds are formulated as  $[\text{Ni}^{\text{III}}_{1-x}\text{Co}^{\text{III}}_x(\text{chxn})_2\text{Br}]\text{Br}_2$ . The other possibility is that the energy level of the  $d_{z^2}$  LH band of Co is lower than that of the  $p_z$

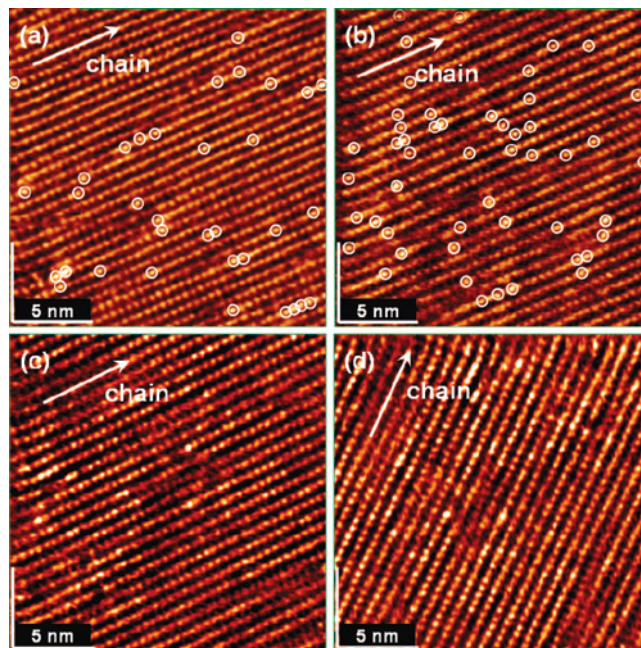


**Figure 5.** STM images of  $[\text{Ni}_{1-x}\text{Co}_x(\text{chxn})_2\text{Br}]\text{Br}_2$  with (a)  $x = 0.01$ , (b)  $x = 0.02$ , (c)  $x = 0.05$ , and (d)  $x = 0.11$  on the  $bc$  plane ( $200 \times 200 \text{ \AA}$ ). The sample bias was  $V_s = +0.25$  V. The 1D chain directions are shown as white arrows. The brighter spots in parts a and b are highlighted with white circles.

band of the bridging Br (Figure 4c). In this case, Co ions are in the  $d^7$  (divalent) state, and holes are doped into the  $p_z$  band of the bridging Br ions. Therefore, these compounds are formulated as  $[\text{Ni}^{\text{III}}_{1-x}\text{Co}^{\text{II}}_x(\text{chxn})_2\text{Br}^{x-1}]\text{Br}_2$ . We excluded the latter possibility because we synthesized the compounds by electrochemical oxidation of the mixed solution of divalent  $[\text{Ni}^{\text{II}}(\text{chxn})_2]\text{Br}_2$  and trivalent  $[\text{Co}^{\text{III}}(\text{chxn})\text{Br}]\text{Br}$ . Therefore, we concluded that these compounds are formulated as  $[\text{Ni}^{\text{III}}_{1-x}\text{Co}^{\text{III}}_x(\text{chxn})_2\text{Br}]\text{Br}_2$ , and the band structure of these compounds are shown in Figure 4b.

To determine the local doped state of  $[\text{Ni}_{1-x}\text{Co}_x(\text{chxn})_2\text{Br}]\text{Br}_2$ , we carried out STM measurements on these mixed metal complexes by using single crystals at room temperature. The sample bias was chosen to be  $V_s = +0.25$  V for  $x = 0.01$ , 0.02, 0.05, and 0.11. Figure 5 shows STM images of the complexes with (a)  $x = 0.01$ , (b)  $x = 0.02$ , (c)  $x = 0.05$ , and (d)  $x = 0.11$  in an area of  $200 \times 200 \text{ \AA}$ . Every spot in the image observed was about  $5 \times 7 \text{ \AA}$ . Because the M–M ( $M = \text{Co}$  or  $\text{Ni}$ ) distances along the  $b$  (1D chain) and  $c$  axes are about  $5.2 \text{ \AA}$  and  $7.1 \text{ \AA}$ , respectively, these spots reflect the periodicity of the  $[\text{M}(\text{chxn})_2]$  units on the  $bc$  plane. Some brighter spots were also observed, and the number of the spots is consistent with the amounts of doped  $\text{Co}^{\text{III}}$  ions. These brighter spots are highlighted with white circles in Figure 5a,b. Therefore, we can assign the brighter spots to  $\text{Co}^{\text{III}}$  sites.

Because the STM measurements were performed with a positive sample bias, the tunnel current is observed from the Fermi energy ( $E_F$ ) of the tip to the conduction band of the sample. In  $[\text{Ni}_{1-x}\text{Co}_x(\text{chxn})_2\text{Br}]\text{Br}_2$ , the conduction band is considered to be composed of the  $d_{z^2}$  orbital of the Ni and Co species. Because Co sites afford brighter spots than Ni

- (11) Yamashita, M.; Takaishi, S. *Bull. Chem. Soc. Jpn.* **2006**, *79*, 1820–1833.  
 (12) Okamoto, H.; Shimada, Y.; Oka, Y.; Chainani, A.; Takahashi, T.; Kitagawa, H.; Mitani, T.; Toriumi, K.; Inoue, K.; Manabe, T.; Yamashita, M. *Phys. Rev. B* **1996**, *54*, 8438–8445.  
 (13) (a) Okamoto, H.; Mitani, T.; Toriumi, K.; Yamashita, M. *Mater. Sci. Eng., B* **1992**, *13*, L9–L14. (b) Okamoto, H.; Mitani, T. *Prog. Theor. Phys.* **1993**, *113*, 191–201.  
 (14) Nasu, K. *J. Phys. Soc. Jpn.* **1984**, *52*, 3865–3873. (b) Iwano, K.; Nasu, K. *J. Phys. Soc. Jpn.* **1992**, *61*, 1380–1389. (c) Webber-Milbrodt, S. M.; Gammel, J. T.; Bishop, A. R.; Lor, E. Y., Jr. *Phys. Rev. B* **1992**, *45*, 6435–6458.

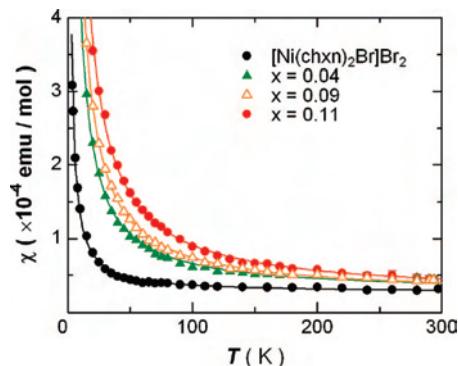


**Figure 6.** Spin susceptibility of  $[\text{Ni}_{1-x}\text{Co}_x(\text{chxn})_2\text{Br}]\text{Br}_2$  with  $x = 0.00$  (black),  $x = 0.02$  (green),  $x = 0.05$  (orange), and  $x = 0.11$  (red). The solid lines are fitting curves by the summation of the Curie spin ( $1/T$ ) and the temperature independent components.

sites with a small bias (+0.25 V), the bottom of the conduction band is considered to be mainly contributed from the Co species, which is in good agreement with the proposed band structure derived from optical data (Figure 4b).<sup>9</sup>

The ESR spectra have been measured using polycrystalline samples. Figure 6 shows the temperature dependence of the spin susceptibility obtained by integrating the ESR signal twice. Spin susceptibility of  $[\text{Ni}_{1-x}\text{Co}_x(\text{chxn})_2\text{Br}]\text{Br}_2$  can be well fitted by the summation of the Curie spin ( $1/T$ ) and the temperature independent contribution. The Curie spin concentration ( $N_c$ ) gradually increased with increasing  $x$  ( $N_c = 0.34\%$ ,  $1.18\%$ ,  $1.58\%$ , and  $2.07\%$  for  $x = 0, 0.04, 0.09$ , and  $0.11$ , respectively). This result can be explained as follows. In the  $[\text{Ni}(\text{chxn})_2\text{Br}]\text{Br}_2$ , it has been clarified that the origin of the Curie spin component is in the free spins of the  $\text{Ni}^{\text{III}}$

species at the chain ends originating in the scission of the 1D chain by the some defects (e.g.,  $\text{Ni}^{\text{II}}$  impurities in a low-spin state). In the case of  $[\text{Ni}_{1-x}\text{Co}_x(\text{chxn})_2\text{Br}]\text{Br}_2$ , low-spin  $\text{Co}^{\text{III}}$  species cut the 1D chains, resulting in the increase of  $N_c$ . Thus, a monotonic increase of  $N_c$  suggests the good substitution of nonmagnetic  $\text{Co}^{\text{III}}$  ions to magnetic  $\text{Ni}^{\text{III}}$  sites in the present materials.

In summary, we have studied the electronic structure of Co doped state in the halogen-bridged Ni–Co mixed metal complexes,  $[\text{Ni}_{1-x}\text{Co}_x(\text{chxn})_2\text{Br}]\text{Br}_2$  by optical, STM, and ESR methods. The optical reflectivity spectrum showed the new band at about 0.5 eV, which is reasonably recognized as the  $d_{z^2}$  band of doped  $\text{Co}^{\text{III}}$  ions. In the STM images, some brighter spots can be assigned to  $\text{Co}^{\text{III}}$  sites. Because we acquired the STM images of  $[\text{Ni}_{1-x}\text{Co}_x(\text{chxn})_2\text{Br}]\text{Br}_2$  with a lower sample bias (+0.25 V) than that of pure Ni compound (+1.3 V), the bottom of the conduction band, which is mainly composed of the  $d_{z^2}$  band of Co ions, is contributed to the tunnel current. This consideration is consistent with the optical data of  $[\text{Ni}_{1-x}\text{Co}_x(\text{chxn})_2\text{Br}]\text{Br}_2$ , that shows a lower band gap energy (0.5 eV) than that of  $[\text{Ni}(\text{chxn})_2\text{Br}]\text{Br}_2$ . In the ESR spectra, the Curie spin concentration was gradually increased with increasing  $\text{Co}^{\text{III}}$  ions, which is explained by the scissions of the  $S = 1/2$  1D antiferromagnetic chains.

**Acknowledgment.** This work was partly supported by a Grant-in-Aid for Creative Scientific Research from the Ministry of Education, Culture, Sports, Science, and Technology.

IC7012232